Journal of Low Temperature Physics (2022) 209:1128–1134
https://doi.org/10.1007/s10909-022-02743-7

Improving the Quality of $CaWO_4$ Target Crystals for CRESST

A. Kinast[1] · G. Angloher[2] · G. Benato[3] · A. Bento[2,9] · A. Bertolini[2] · R. Breier[4] · C. Bucci[3] · L. Canonica[2] · A. D'Addabbo[3] · S. Di Lorenzo[3] · L. Einfalt[5,6] · A. Erb[1,11] · F. V. Feilitzsch[1] · N. Ferreiro Iachellini[2] · S. Fichtinger[5] · D. Fuchs[2] · A. Fuss[5,6] · A. Garai[2] · V.-M. Ghete[5] · P. Gorla[3] · S. Gupta[5] · F. Hamilton[1] · D. Hauff[2] · M. Ješkovský[4] · J. Jochum[7] · M. Kaznacheeva[1] · H. Kluck[5] · H. Kraus[8] · A. Langenkämper[1] · M. Mancuso[2] · L. Marini[3] · V. Mokina[5] · A. Nilima[2] · M. Olmi[3] · T. Ortmann[1] · C. Pagliarone[3,12] · V. Palušová[4] · L. Pattavina[1,10] · F. Petricca[2] · W. Potzel[1] · P. Povinec[4] · F. Pröbst[2] · F. Pucci[2] · F. Reindl[5,6] · J. Rothe[1] · K. Schäffner[2] · J. Schieck[5,6] · D. Schmiedmayer[5,6] · S. Schönert[1] · C. Schwertner[5,6] · M. Stahlberg[2] · L. Stodolsky[2] · C. Strandhagen[7] · R. Strauss[1] · I. Usherov[7] · F. Wagner[5,6] · M. Willers[1] · V. Zema[2] · CRESST Collaboration

Received: 29 October 2021 / Accepted: 26 April 2022 / Published online: 24 May 2022

Abstract

The Cryogenic Rare Event Search with Superconducting Thermometers (CRESST) experiment aims at the direct detection of dark matter particles via their elastic scattering off nuclei in a scintillating $CaWO_4$ target crystal. The $CaWO_4$ crystal is operated together with a light detector at mK temperature and read out by a Transition Edge Sensor. For many years, $CaWO_4$ crystals have successfully been produced in-house at Technical University of Munich (TUM) with a focus on high radiopurity which is crucial to reduce background originating from radioactive contamination. In order to further improve the $CaWO_4$ crystals, an extensive chemical purification of the raw materials and the synthesised $CaWO_4$ powder has been performed. In addition, a temperature gradient simulation of the growth process and subsequently an optimisation of the growth furnace with the goal to reduce the intrinsic stress was carried out. We present results on the intrinsic stress in the $CaWO_4$ crystals and on the $CaWO_4$ powder radiopurity. A crystal grown from the purified material was installed in the current CRESST set-up. The detector is equipped with an instrumented holder which is used to measure the alpha decay rate of the crystal. We present a preliminary analysis showing a significantly reduced intrinsic background from natural decay chains.

Keywords CRESST · $CaWO_4$ · Crystal growth · Radiopurity

✉ A. Kinast
angelina.kinast@tum.de

Extended author information available on the last page of the article

1 The CRESST-III Experiment

Cryogenic Rare Event Search with Superconductive Thermometers (CRESST) [1] aims at the direct detection of dark matter (DM) using cryogenic calorimeters. The latest CRESST-III module consists of a scintillating 24 g $CaWO_4$ single crystal as target material. It is operated at ~ 10 mK temperatures and equipped with a Transition Edge Sensor (TES) for a precise measurement of the energy deposited by a particle interaction within the crystal. In addition to the $CaWO_4$ crystal, a light detector (LD), also equipped with a TES, is read out in coincidence. This enables discrimination between electromagnetic interactions (background-like events), alpha decays (background events, less relative scintillation light) and nuclear recoils (signal-like events, least relative scintillation light) due to the different relative fraction of scintillation light produced. CRESST-III detectors reach thresholds as low as 30.1 eV [1], allowing a very sensitive measurement of particle recoil energies. One key point for the excellent performance of these detectors is the quality of the target crystals. This includes the quality of the crystal lattice in terms of stress or defects, as well as a high radiopurity of the $CaWO_4$ material itself to minimise backgrounds resulting from natural decay chains. Beta decays, especially, can cause events in the region of interest for DM search. To assure the high quality of the $CaWO_4$ crystals, they have been produced in-house at Technische Universität München (TUM) for many years [2]. In this way, every step of the production is controlled and optimised. A milestone was the production of the crystal TUM40 operated in CRESST-II which showed an excellent performance and a lower background compared to commercially purchased crystals operated in the same CRESST run. It was, up to now, the most radiopure TUM grown crystal [3]. To further improve the crystal quality, two different approaches are followed at TUM: the reduction of intrinsic stress caused by temperature gradients during crystal growth and a chemical purification of the raw materials and the $CaWO_4$ powder. Both are described in the following sections.

2 Reduction of Intrinsic Stress in $CaWO_4$

The $CaWO_4$ crystals are grown via the Czochralski principle from $CaWO_4$ powder which is heated up to its melting point at ~ 1620 °C. A small $CaWO_4$ crystal, the so-called seed crystal, is lowered into the liquid $CaWO_4$ melt until it touches the melt surface and moved upward again under rotation. At the contact area, the crystal forms with the same crystal orientation as the seed crystal. For this growth technique, it is important that the temperature gradient in the melt is well controlled. A too large gradient can cause a non-intended crystallisation below the surface of the melt, forming a cone along the isotherms. This formation of the cone causes stress in the crystal lattice. In order to minimise these effects, a simulation of the furnace and the temperature gradients during growth was performed using COMSOL multiphysics [4]. The simulation showed that a heat radiation shield above the crucible and an extra heating disc below the crucible lead to gradient reduction [5]. To confirm the results from the simulation, the furnace was modified accordingly by installing the heat radiation disc and the extra heating disc at the bottom. A test crystal (growth number TUM89) was grown in this set-up.

In order to quantify the reduction of stress, two crystal slices were compared in a photoelasticity measurement. The experimental set-up (Fig. 1 *Left*) consists of a white light source, a polariser, the sample, an analyser and a CCD (charge-coupled device) camera. It is used to determine the stress distribution in a transparent sample trough stress birefringence. The polarised light which goes through the sample is divided into wave components along the principal stress axes. The different refractive indices caused by the intrinsic stress lead to phase shifts of the light. The light passes the analyser polarisation filter and is recorded by the CCD camera. This method allows to qualitatively compare two samples by comparing the stress patterns in both. The finer the pattern is, the more stress is in the crystal lattice. Figure 1 *Middle/Right* shows a comparison of the crystal TUM73 which was grown in the Czochralski furnace prior to the furnace modifications, with the crystal TUM89 which was produced with the modifications in place. The pictures are colour coded to highlight the difference in the recorded pattern. Crystal TUM73 shows more small artefacts in its middle implying that the polarisation was shifted a couple of times. In comparison with it, crystal TUM89 only shows one bright pattern at the edges of the crystal, which is expected as the crystal is growing with round edges, whereas the underlying crystal lattice is tetragonal, leading to surface tensions. For this crystal, the polarisation was only shifted once. Hence, the modifications described above helped to decrease the intrinsic stress in TUM89.

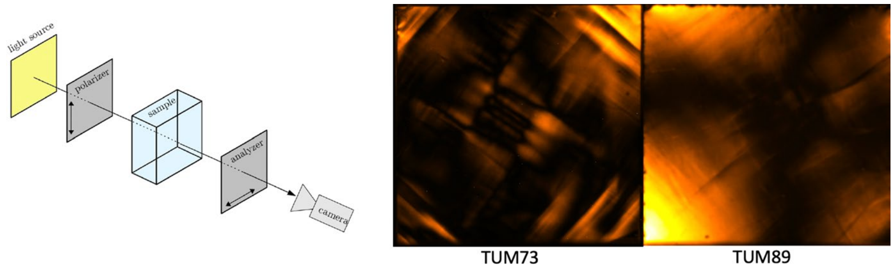

Fig. 1 *Left* Photoelasticity set-up at TUM. It consists of a white light source, a polariser, the sample, an analyser and a CCD camera. *Middle* and *Right* Comparison of the crystals TUM73 (grown before modifications of the furnace) and TUM89 (grown after modifications). TUM73 shows a finer structure in the middle of the crystal, whereas TUM89 has only one major structure visible at its edges. (Colour figure online)

3 $CaWO_4$ Purification

Recently, an extensive chemical purification of the raw materials $CaCO_3$ and WO_3 using liquid–liquid extraction and coprecipitation methods, and a novel production method of $CaWO_4$ via a precipitation reaction and a washing procedure of the synthesised $CaWO_4$ powder have been developed at TUM with the goal to increase the radiopurity of the crystals. Measurements of the powder using HPGe-detectors show promising results concerning the radiopurity of the powder [6]. However, HPGe-measurements are not sensitive enough for the current purity level, as they only give upper limits. Hence, a more sensitive measurement is needed, which is the operation of the $CaWO_4$ crystal as a cryogenic detector. In August 2019, the crystal TUM93 was grown from the chemically purified powder in the stress optimised Czochralski set-up (see Sect. 2) at TUM and cut into three CRESST-shaped (20 mm × 20 mm × 10 mm, 24 g) crystals named TUM93A, TUM93B, TUM93C, with TUM93A being the crystal from the top of the ingot. Due to segregation effects during crystal growth, the topmost part of the crystal is the cleanest part in terms of radiopurity [6].

4 Radiopurity of the Crystal TUM93A

For the detector crystal TUM93A, the standard detector module design was modified in a way that enables to detect alpha decays occurring in the crystal. This is important as the standard CRESST design is optimised to detect sub-keV energies (thresholds as low as 30.1 eV [1]); therefore, an MeV alpha decay signal is completely out of the linear region of the detector. To enable both, a low threshold dark matter detector and a possibility to detect alpha decays, one of the holding sticks of the crystal is also made from another TUM grown $CaWO_4$ crystal and instrumented with its own TES. When an event happens in the main $CaWO_4$ crystal, a small percentage of the signal is transmitted via the point-like contact of the $CaWO_4$ crystal to the instrumented stick (i-stick) and can be read out by the

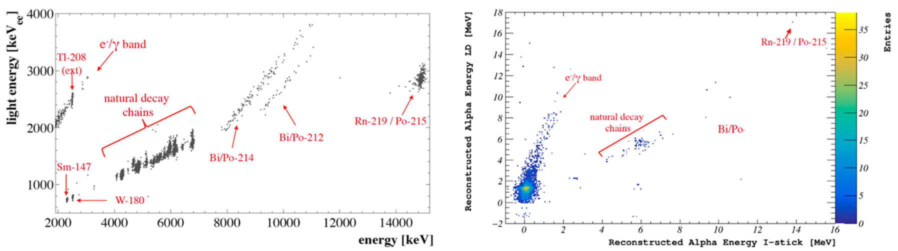

Fig. 2 *Left* Plot with the TUM40 results [3] for reference. The plot zooms in to the alpha region and outlines the different areas. On the left end decays from ^{147}Sm and ^{180}W are located followed by the single line natural decay chains, alpha/beta coincidences (^{214}Bi/^{214}Po and ^{212}Bi/^{212}Po) and alpha/alpha coincidences ^{219}Rn/^{215}Po. *Right* Results of TUM93 showing the detected signal from the i-stick on the *x*-axis and the detected light signal on the *y*-axis. The 2D-histogram shows the alpha band and highlights the same regions as the TUM40 plot. (Colour figure online)

i-stick TES. In addition to this signal, the LD is read out in coincidence to enable particle discrimination (see Sect. 1). Up to now 2012 h of data corresponding to an exposure of 2.01 kg days exposure have been analysed and compared to the results from the crystal TUM40 from [3] which was the previous best TUM crystal in terms of radiopurity. As described in Sect. 1, alpha events have less relative scintillation light compared to electromagnetic interactions and hence have their own band in a light vs phonon energy plot. Figure 2 shows these bands for the crystal TUM40 (*Left*) as reference vs. the crystal TUM93A (*Right*), where the TUM93A plot shows the energy detected by the i-stick on the x-axis and the LD on the y-axis.

In total, 93 alpha decays have been detected for TUM93A so far. The alphas can be assigned to 4 different regions in the plot following the TUM40 alpha analysis [3]. From 2 to 4 MeV, ^{147}Sm and ^{180}W alpha decays are located. Between 4 and 7 MeV, the alpha lines from single decays originating from the three natural decay chains (^{238}U, ^{235}U and ^{232}Th) are situated. Between 7 and 12 MeV, cascades from the coincident alpha and beta decays from ^{214}Bi/^{214}Po and ^{212}Bi/^{212}Po are found. Above 14 MeV, the double alpha coincidences from the ^{219}Rn/^{215}Po decay can be seen. For the TUM93A data, the ^{147}Sm events were used for the energy calibration of the i-stick and the LD. Table 1 shows the results for the different alpha event classes, the total alpha decay rate and the alpha decays originating from the natural decay chains. The alpha decay rate of the natural decay chains is $489 \pm 53 \frac{10^{-6}}{\text{s}\cdot\text{kg}}$. In comparison, the crystal TUM40 showed an alpha decay rate of $3080 \frac{10^{-6}}{\text{s}\cdot\text{kg}}$ which means that the radiopurity of TUM93 has been increased by a factor of 6.3 ± 0.7.

Table 1 Decay rates of different parts of the alpha band

	Number of events	Decay rate $\left[\frac{10^{-6}}{\text{s}\cdot\text{kg}}\right]$
Total α decay rate	93	535 ± 55
^{147}Sm and ^{180}W	8	46 ± 16
SINGLE α lines (nat. decay chains)	79	454 ± 51
^{214}Bi/^{214}Po and ^{212}Bi/^{212}Po cascades (nat. decay chain)	5	29 ± 13
^{219}Rn–^{215}Po decay (nat. decay chain)	1	6
Total α decay rate nat. decay chains	85	489 ± 53

In total, 93 alpha events were observed in the analysed data. The total alpha decay rate is formed by the rates from ^{147}Sm and ^{180}W which do not originate from the thorium and uranium decay chains and the other decays from these natural decay chains, with single alpha lines between 4 MeV and 8 MeV. The coincident alpha/gamma decays of $^{214/212}$Bi/$^{214/212}$Po occur in cascades. The coincident alpha/alpha decays from ^{129}Rn/^{215}Po are detected above 14 MeV. The errors are statistic errors, and simulations were performed to account for systematic errors and a correction for trigger- and cut-efficiencies

5 Summary

The CRESST experiment requires high-quality $CaWO_4$ crystals for dark matter search. These crystals have been successfully produced at TUM for many years with a higher quality than any commercially available $CaWO_4$ crystals. In the last years, the intrinsic stress of the crystals originating from the temperature gradients during the growth process has been reduced via a modification of the Czochralski growth furnace following a temperature gradient simulation. An extensive $CaWO_4$ powder purification was developed and applied to $CaWO_4$ powder and raw materials, improving radiopurity as obtained by HPGe screening results. The crystal TUM93 was grown from this powder and is currently operated in CRESST as a dark matter detector. The implementation of an instrumented holding stick in this detector enables the detection of alpha decays. The detector TUM93A shows a total alpha rate originating from natural decay chains of $489 \pm 53 \, \frac{10^{-6}}{\mathrm{s \cdot kg}}$ which is a reduction by a factor 6.3 ± 0.7 compared to the previous best crystal TUM40.

Acknowledgements This research has been supported by the DFG cluster of excellence "Origin and Structure of the Universe" and the "Origins" cluster, by the BMBF Verbundprojekt 05A2017 CRESST-XENON and by the SFB1258. We would also like to thank IKZ Berlin for their help with the COMSOL crystal growth simulations.

Funding Open Access funding enabled and organized by Projekt DEAL.

Data availability The datasets generated during and/or analysed during the current study are not yet publicly available, but will be available from the corresponding author on reasonable request.

References

1. A.H. Abdelhameed et al., First results from the CRESST-III low-mass dark matter program. Phys. Rev. D **100.10**, 102002 (2019). https://doi.org/10.1103/PhysRevD.100.102002
2. A. Erb, J.C. Lanfranchi, Growth of high-purity scintillating $CaWO_4$ single crystals for the low-temperature direct dark matter search experiments CRESST-II and EURECA. Cryst. Eng. Commun. **15**(12), 2301–2304 (2013). https://doi.org/10.1039/c2ce26554k
3. R. Strauss et al., Beta/gamma and alpha backgrounds in CRESST-II Phase 2. JCAP (2015). https://doi.org/10.1088/1475-7516/2015/06/030
4. COMSOL Multiphysics® v. 5.3. www.comsol.com. COMSOL AB, Stockholm, Sweden
5. F. Hamilton, Simulation der Temperaturverteilung während der Züchtung von $CaWO_4$ Kristallen für CRESST an der Czochralski-Anlage der TUM (Technische Universität München, Bachelor-thesis, 2019)

6. A. Münster, High-purity $CaWO_4$ single crystals for direct dark matter search with the CRESST Experiment (Technische Universität München, Ph.D.-thesis, 2017)

Publisher's Note Springer Nature remains neutral with regard to jurisdictional claims in published maps and institutional affiliations.

Authors and Affiliations

A. Kinast[1] · G. Angloher[2] · G. Benato[3] · A. Bento[2,9] · A. Bertolini[2] · R. Breier[4] · C. Bucci[3] · L. Canonica[2] · A. D'Addabbo[3] · S. Di Lorenzo[3] · L. Einfalt[5,6] · A. Erb[1,11] · F. V. Feilitzsch[1] · N. Ferreiro Iachellini[2] · S. Fichtinger[5] · D. Fuchs[2] · A. Fuss[5,6] · A. Garai[2] · V.-M. Ghete[5] · P. Gorla[3] · S. Gupta[5] · F. Hamilton[1] · D. Hauff[2] · M. Ješkovský[4] · J. Jochum[7] · M. Kaznacheeva[1] · H. Kluck[5] · H. Kraus[8] · A. Langenkämper[1] · M. Mancuso[2] · L. Marini[3] · V. Mokina[5] · A. Nilima[2] · M. Olmi[3] · T. Ortmann[1] · C. Pagliarone[3,12] · V. Palušová[4] · L. Pattavina[1,10] · F. Petricca[2] · W. Potzel[1] · P. Povinec[4] · F. Pröbst[2] · F. Pucci[2] · F. Reindl[5,6] · J. Rothe[1] · K. Schäffner[2] · J. Schieck[5,6] · D. Schmiedmayer[5,6] · S. Schönert[1] · C. Schwertner[5,6] · M. Stahlberg[2] · L. Stodolsky[2] · C. Strandhagen[7] · R. Strauss[1] · I. Usherov[7] · F. Wagner[5,6] · M. Willers[1] · V. Zema[2] · CRESST Collaboration

[1] Physik-Department and Excellence Cluster Origins, Technische Universität München, 85747 Garching, Germany

[2] Max-Planck-Institut für Physik, 80805 Munich, Germany

[3] Laboratori Nazionali del Gran Sasso, INFN, 67100 Assergi, Italy

[4] Faculty of Mathematics, Physics and Informatics, Comenius University, 84248 Bratislava, Slovakia

[5] Institut für Hochenergiephysik der Österreichischen Akademie der Wissenschaften, 1050 Wien, Austria

[6] Atominstitut, Technische Universität Wien, 1020 Wien, Austria

[7] Eberhard-Karls-Universität Tübingen, 72076 Tübingen, Germany

[8] Department of Physics, University of Oxford, Oxford OX1 3RH, UK

[9] Departamento de Fisica, Universidade de Coimbra, P3004 516 Coimbra, Portugal

[10] GSSI-Gran Sasso Science Institute, 67100 L'Aquila, Italy

[11] Walther-Meißner-Institut für Tieftemperaturforschung, 85748 Garching, Germany

[12] Dipartimento di Ingegneria Civile e Meccanica, Universitá degli Studi di Cassino e del Lazio Meridionale, 03043 Cassino, Italy